

# Attitude Control Mechanism in an Insect-like Tailless Two-winged Flying Robot by Simultaneous Modulation of Stroke Plane and Wing Twist

H.V. Phan<sup>1</sup>, S. Aurecianus<sup>2</sup>, T. Kang<sup>2</sup> and H.C Park<sup>1\*</sup>

<sup>1</sup>Artificial Muscle Research Center and Department of Smart Vehicle Engineering, Konkuk University, Seoul 05029, South Korea

<sup>2</sup>Department of Aerospace Information Engineering, Konkuk University, Seoul 05029, South Korea

## ABSTRACT

In an insect-like tailless flying robot, flapping wings should be able to produce control force as well as flight force to keep the robot staying airborne. This performance requires an active control mechanism that produces sufficient control torques to stabilize the robot due to the inherent instability. In this work, we propose a control mechanism integrated in a hovering-capable, two-winged, flapping-wing, 17.6 g flying robot (KUBeetle-S) that can simultaneously change the wing stroke-plane and wing twist. The mechanism is capable of tilting the stroke plane causing change in the wing twist to produce coupling control torques for pitch and roll. For yaw (heading change), the root spars of the left and right wings are adjusted asymmetrically to change the wing twist during flapping motion, resulting in yaw torque generation. We first performed a series of experiments using a 6-axis force/torque load cell to evaluate the effectiveness of the control mechanism via torque generation. We then prototyped the robot integrating the control mechanism with sub-micro servos as actuators and flight control board, and conducted free flight tests to verify the possibility of attitude control.

## 1 INTRODUCTION

In the absence of tail control surface, insects are capable of modifying their wing kinematics to produce control forces for attitude change during flight [1,2]. In particular, shifting the stroke plane position or flapping angle ranges for pitch response was found in fruit fly *Drosophila melanogaster* [3] and hoverflies *Eristalis tenax* and *Episyrphus balteatus* [4]. For roll and yaw responses, many insect species such as *Drosophila spp.* [5], *Musca domestica* [6], *Calliphora spp.* [7], dragonflies [8], beetles [9], and hawkmoths [10], are found to change their flapping amplitudes of two wings.

Mimicking those complex kinematics manipulation abilities is a challenging task in developing light-weight insect-like tailless flapping-wing flying robots. Without tail stabilizer, the main flapping wings should be incorporated with a control mechanism to produce control forces as well as sufficient flight force to keep the robot staying airborne. Within a limited takeoff weight of the robot, a proposed control mechanism should be fitted for light-weight actuators, which generate a low actuation torque. Additionally, the mechanism is also required to produce enough control torques for attitude changes. Due to the hurdles, there are only a few hovering tailless flying robots ready for free flight although many research groups have successfully developed bird-like tailed robots [11-15]. A 19 g Nano Hummingbird developed by AeroVironment

[16] is the first tailless two-winged robot that successfully performs stable controlled flight. It utilizes a wing twist modulation mechanism by controlling the wing root spars symmetrically or asymmetrically for roll, pitch, and yaw controls. Similar wing twist modulation mechanism can be found in a 21 g KUBeetle [17] and a 22 g Colibri robot [18]. Otherwise, wing kinematics modulation was used as a control approach in a tiny 80 mg Robobee [19] and a 12 g robotic hummingbird [20]. In this approach, wing stroke amplitudes of the left and right wings are changed asymmetrically for roll control. By shifting the mean stroke angle of the two wings forward or aft, pitch control is obtained. In addition, modulation of stroke velocities in each half-stroke within a flapping cycle results in a yaw torque generation for yaw control. Another flight control approach is the wing stroke-plane modulation for pitch and yaw controls used in a 62 g Robotic Hummingbird [21].

We have been also developing a tailless flying robot KUBeetle, which performed stable flight for about 40 s [17]. We have tested for many control approaches including modulations of mean stroke angle [22], stroke-plane angle [23], or wing twist [17]. However, these control mechanisms were complicated for fabrication and required high-torque actuators. In this work, we propose a simple and lightweight control mechanism that is able to modify synchronously the stroke plane and wing twist for attitude changes. We design and fabricate the mechanism, and evaluate its possibility of control force and torque generation using a 6-axis force/torque load cell. Then, the control mechanism, which is actuated by three micro servos, is integrated in the flying robot for free controlled flight test.

## 2 FLAPPING-WING MECHANISM

The tailless robot is developed aiming to mimic the flight of a horned beetle, *Allomyrina Dichotoma*, who is capable of hovering flight. Since the mechanical design of the flapping-wing

mechanism was presented in detail in [17], this paper shows only a brief summary. Two deformable wings are actuated by a 3.5 g coreless motor (Chaoli CL720, China) through a gearbox (24:1) to amplify the torque of the motor and a transmission linkage system, which converts the rotary motion to the flapping motions using a combined operation of the 4-bar linkage and the pulley-string mechanism. The wing with a length of 75 mm was made of 10  $\mu\text{m}$  Mylar film as wing membranes and one-layer carbon strips as reinforced veins. After installing to the flapping mechanism, the two wings are able to deform creating spanwise twist and chordwise camber during the flapping motion [16]. Flapping amplitude is approximately 190° allowing the presence of clap-and-fling effect for vertical force augmentation [24]. Effect of vein structures on force generation and power requirement was also investigated [25].

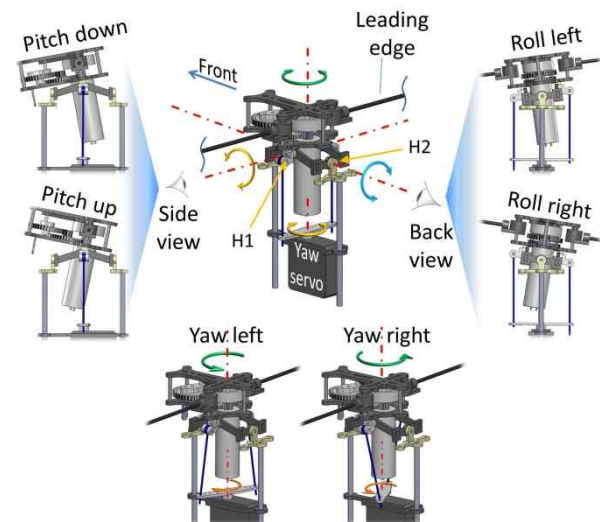


Figure 1 – Conceptual design of the control mechanism for attitude change.

## 3 ATTITUDE CONTROL MECHANISM

### 3.1 Conceptual design and fabrication

Figure 1 shows CAD images of the flight control mechanisms for pitch, roll and yaw attitude changes. The flapping-wing mechanism (including the motor) is able to rotate about two hinges (H1 and H2 in Figure 1) for pitch and roll controls. By tilting the flapping-wing mechanism around the

hinge H1 forward or backward, the wing stroke plane is tilted in the same direction to the change in the directions of forces for pitch torque generation. Additionally, since the wing root spars are fixed, in this case, tilting the stroke plane causes the modulation in wing twist to produce additional pitch torque. To generate roll control torque, the flapping-wing mechanism is rotated about hinge H2 to tilt the stroke plane laterally to the left or right (Figure 1). As a result, wing twists of the two wings are also modulated asymmetrically. Thus, pitch and roll control torques are generated by simultaneously changing the stroke plane and modulating the wing twist. Yaw motion is controlled by rotating the root spars of the left and right wings in the opposite directions, as shown in Figure 1.

Based on the conceptual design, we fabricated the control mechanism using a 0.8 mm carbon/epoxy panel and installed in the flying robot, as depicted in Figure 2. Pitch and yaw controls are actuated independently by two conventional ultra-micro digital servos (HK-5320, hobbyking.com) weighing 1.5 g. Meanwhile, roll control is actuated by a sub-micro LZ servo (0.5 g, microflierradio.com).

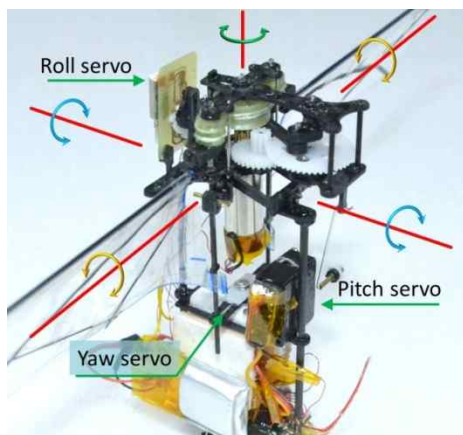


**Figure 2 - Prototype of the control mechanism integrated in the flying robot.**

### 3.2 Force and torque generation

To investigate the capability of control torques generation, we set up an experiment using a 6-axis load cell (Nano 17, ATI Industrial Automation, USA, force resolution  $\approx 0.3$  gf, torque resolution  $\approx$

0.0156 N.mm), as shown in Figure 3. We located the load cell close to the location of the robot's center of gravity (CG). Thus, the torques obtained from the load cell can be regarded as those about the CG. We powered the flapping-wing system using an external power supply (E36103A, Keysight, Korea) at a flapping frequency of 23 Hz.

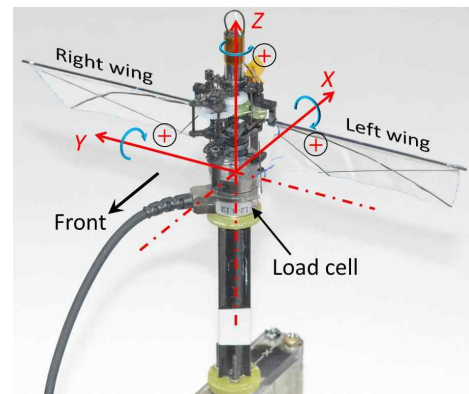


**Figure 3 – Experimental setup for forces and torques measurement using a load cell**

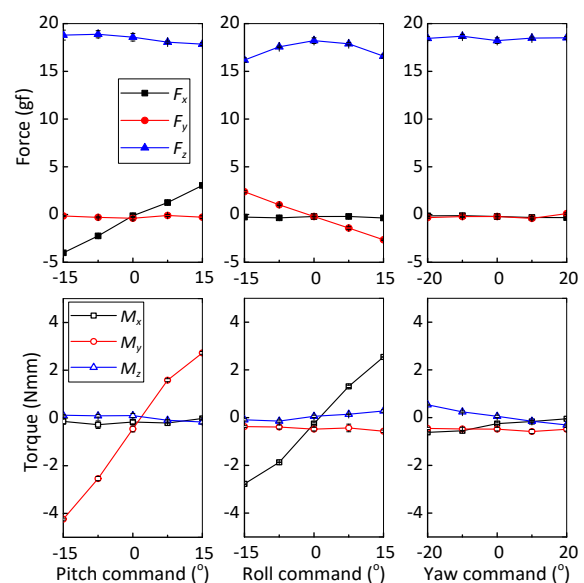


**Figure 4 – Generation of forces and torques in three axes for a range of control inputs.**

Figure 4 shows the forces and torques generated in all three axes for different pitch, roll and yaw inputs. At 23 Hz, a vertical force of about 18.5 gf was produced. Changing control inputs for pitch resulted in linear changes in horizontal force and pitch torque. In the range of control input (stroke-plane angle) from  $-15^\circ$  (pitch down) to  $15^\circ$  (pitch up), the measured horizontal force varied from  $-4.0$  gf to  $3.1$  gf and pitch torque varied from  $-4.2$

N.mm to 2.7 N.mm. With no control inputs for hovering condition, pitch torque of about -0.5 Nmm was generated. This is due to slight vertical misalignment between the mean aerodynamic force center and the load cell. Effect of pitch control inputs on other force and torque signals was insignificant. For roll control, changing the control input from -15° (roll right) to 15° (roll left) resulted in the changes of lateral force from 2.4 gf to -2.6 gf, and roll torque from -2.8 N.mm to 2.6 N.mm. A slight decrease in the vertical force was found for a higher roll command angle. Yaw torque is less sensitive to the yaw command compared to those of pitch and roll commands. For the range of yaw inputs by the tilt of yaw servo's arm (Figure 1) from -20° to 20°, yaw torque varied from 0.5 N.mm to -0.3 N.mm (a reference of 0.06 N.mm at hovering condition).

#### 4 FLIGHT EXPERIMENT

##### 4.1 Attitude stabilization

For attitude control and stabilization, a custom-built 1 g control board [26] was mounted onboard. The board consists of a microprocessor ARM Cortex-M4 32-bit STM32L432KC, a 6-axis gyroscope and accelerometer MPU-9250, a 2.4GHz transceiver nRF24L01+, and power regulators, as shown in Figure 5. Due to the inherent instability of the tailless robot, a feedback PD controller was implemented in the control system to sense the attitudes of the robot, which can be determined by the roll, pitch, yaw Euler angles ( $\phi$ ,  $\vartheta$ ,  $\psi$ , respectively), and angular rates ( $p$ ,  $q$ ,  $r$ , respectively) about the X-, Y-, and Z-axis, respectively. Accelerometer readings are used to obtain the roll and pitch angles. Meanwhile, the angular rates are estimated from the gyroscope readings. Thus, the roll and pitch attitudes can be estimated either by an accelerometer or a gyroscope. However, the data obtained from the accelerometers are strongly affected by vibrations caused by a high flapping motion. The gyroscope signals, on the other hand, are less sensitive to disturbances, but drift by

time. To solve this issue, a combination of low-pass and Kalman filters, which uses the signals from both gyroscope and accelerometer, was used to filter the roll and pitch angles, while a low-pass filter was used to smooth the yaw signal [26].

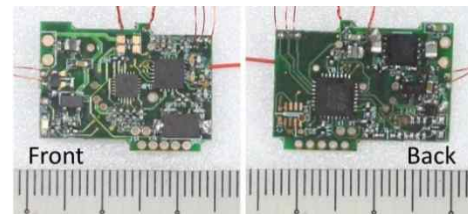


Figure 5 – Custom-built flight control board used in the flying robot.

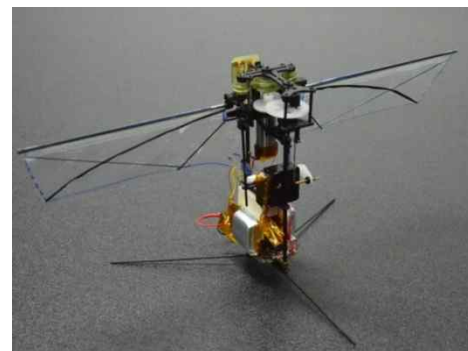


Figure 6 – Overview of the KUBeetle-S integrated with onboard control system.

Component	Weight (g)	Percentage (%)
Flapping mechanism	3.0	17.0
Driving motor	3.5	19.9
Control servos	3.8	21.6
Control mechanism	0.5	2.8
Batteries	4.2	23.9
Control board	1.0	5.7
Supporting frames	0.9	5.1
Wings	0.4	2.3
Wires	0.3	1.7
<b>Total mass</b>	<b>17.6</b>	

Table 1 - Mass breakdown of the KUBeetle-S

##### 4.2 Characteristics of the flying robot

Table 1 shows the weight breakdown of the robot, which is named KUBeetle-S, used for flight. The robot with a wingspan of 170 mm and height of 75 mm (Figure 6) weighs about 17.6 g. The driving motor was powered by a two-cell lithium-polymer battery connected in series (7.4 V, 70 mAh). With



onboard regulators in the control board, the servos and MPU9250 sensor were supplied by 5V and 3.7V sources, respectively. The power inputted to the motor was manually controlled through the power throttle stick.

4.3 Flight tests

The KUBeetle-S was tested for its free flight to evaluate the effectiveness of the control mechanism. We recorded the flight using three synchronized high-speed cameras (Photron Ultima APX, 1024 x 1024 pixels, 250 fps). The flight trajectory and body attitude (roll, pitch, and yaw angles) of the robot were obtained using DLT program [27]. Due to the limitation in the recording time of the high-speed cameras, the flight used for the analysis was lasted in 8 seconds. Figure 7 shows the composite images and trajectory of the robot during its flight. Its body attitude is shown in Figure 8. Pitch and roll angles showed small variations from the reference of 0°. Yaw motion was stabilized using gyroscope signal only, which experience drift during flight. Additionally, yaw control torque is less sensitive to the yaw input, as shown in Figure 4. Therefore, heading direction is drifted during flight. However, the upright stability of the robot was unaffected by the heading stability. With the battery capacity, the robot demonstrated its successful flight for more than 2.5 minutes. The flight thus proved that the attitude control system is successfully implemented in an insect-like tailless flying robot.

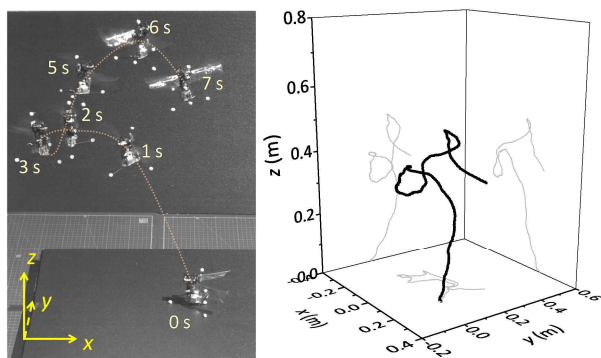


Figure 7 –Composite images and three-dimensional trajectory of the KUBeetle-S during hovering flight.

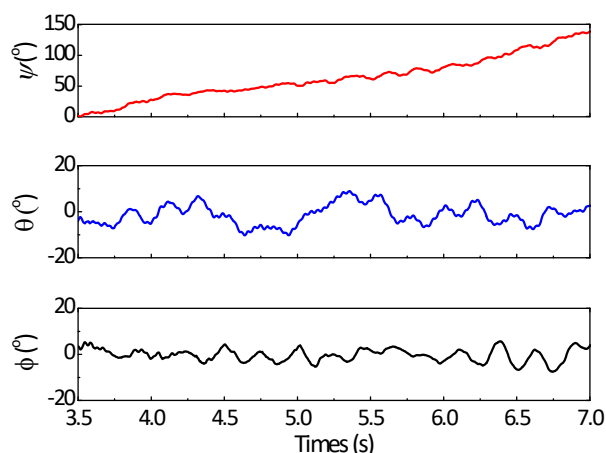


Figure 8 – Attitude performance of the KUBeetle-S during hovering flight.

5 CONCLUSION

This work introduced a 17.6 g insect-like tailless, two-winged, hovering-capable KUBeetle-S robot that can change its stroke plane and wing twist simultaneously for pitch and roll controls, and modulate the wing root spars asymmetrically for yaw control. The proposed control mechanism, which requires less actuation torques from actuators, is simple and easy for fabrication allowing us to use small actuators for saving weight. The measured force and torque proved that the control mechanism can effectively generate reasonable amount of force and torque for attitude changes. Finally, the KUBeetle-S with implementation of onboard attitude feedback control system successfully hovered and loitered for more than 2.5 mins, demonstrating the effectiveness of the proposed control mechanism.

ACKNOWLEDGEMENTS

This research was partially supported by the 2018 KU Brain Pool Program of Konkuk University, Korea.

REFERENCES

[1] R. Dudley. The biomechanics of insect flight: Form, function, evolution. Princeton, NJ: Princeton University Press, 2002.

[2] G. K. Taylor. Mechanics and aerodynamics of insect flight control. Biological Reviews, 76:449-471, 2001.

- [3] J. M. Zanker. On the mechanism of speed and altitude control in *Drosophila melanogaster*. *Physiological Entomology*, 13:351–361, 1988.
- [4] C. P. Ellington. The aerodynamics of hovering insect flight. I. The quasi-steady analysis. *Philosophical Transactions of the Royal Society B*, 305:1-15, 1984.
- [5] S. Vogel. Flight in *Drosophila*. II. Variations in stroke parameters and wing contour. *Journal of Experimental Biology*, 46:383–392, 1967.
- [6] M. V. Srinivasan. A visually-evoked roll response in the housefly. Open-loop and closed-loop studies. *Journal of Comparative Physiology A*, 119:1–14, 1977.
- [7] W. Nachtigall, and W. Roth. Correlations between stationary measurable parameters of wing movement and aerodynamic force production in the blowfly (*Calliphora vicina* R.-D.). *Journal of Comparative Physiology A*, 150:251–260, 1983.
- [8] D. E. Alexander. Unusual phase relationships between the forewings and hindwings in flying dragonflies. *Journal of Experimental Biology*, 109:379–383, 1984.
- [9] A. J. Burton. Directional change in a flying beetle. *Journal of Experimental Biology*, 54:575–585, 1971.
- [10] A. E. Kammer. The motor output during turning flight in a hawkmoth *Manduca sexta*. *Journal of Insect Physiology*, 17:1073–1086, 1971.
- [11] J. H. Park, and K. J. Yoon. Designing a biomimetic ornithopter capable of sustained and controlled flight. *Journal of Bionic Engineering*, 5 (1):39-47, 2008.
- [12] G. C. H. E. de Croon, M. A. Groen, C. D. Wagter, B. Remes, R. Ruijsink, and B. W. van Oudheusden. Design, aerodynamics and autonomy of the DelFly. *Bioinspiration & Biomimetics*, 7:025003, 2012.
- [13] Festo, SmartBird - Aerodynamic lightweight design with active torsion, [https://www.festo.com/net/SupportPortal/Files/46270/Brosch\\_SmartBird\\_en\\_8s\\_RZ\\_110311\\_lo.pdf](https://www.festo.com/net/SupportPortal/Files/46270/Brosch_SmartBird_en_8s_RZ_110311_lo.pdf), 2011.
- [14] S. S. Baek, F. L. G. Bermudez, and R. S. Fearing. Flight control for target seeking by 13 gram ornithopter. In *IEEE Conference on Intelligent Robots and Systems (IROS)*, 2011.
- [15] Q. V. Nguyen, W. L. Chan, and M. Debiasi. Hybrid design and performance tests of a hovering insect-inspired flapping-wing micro aerial vehicle. *Journal of Bionic Engineering*, 13(4):235-248, 2016.
- [16] M. T. Keennon, K. Klingebiel, H. Won, and A. Andriukov. Development of the Nano Hummingbird: A Tailless Flapping Wing Micro Air Vehicle. In *50th AIAA Aerospace Sciences Meeting*, 2012.
- [17] H.V. Phan, T.S. Kang, and H.C. Park. Design and stable flight of a 21 g insect-like tailless flapping wing micro air vehicle with angular rates feedback control. *Bioinspiration & Biomimetics*, 12:036006, 2017.
- [18] A. Roshanbin, H. Altartouri, M. Karásek and A. Preumont. Colibri: A hovering flapping twin-wing robot. *International Journal of Micro Air Vehicles*, 9(4):270-282, 2017.
- [19] K. Y. Ma, P. Chirarattananon, S. B. Fuller, and R. J. Wood. Controlled flight of a biologically inspired insect-scale robot. *Science*, 340:603-607, 2013.
- [20] J. Zhang, Z. Tu, F. Fei, and X. Deng. Geometric flight control of a hovering robotic hummingbird. In *IEEE Conference on Robotics and Automation (ICRA)*, 2017.
- [21] D. Coleman, M. Benedict, and I. Chopra. Design, Development and Flight Testing of Robotic Hummingbird. In *71st Annual Forum of the American Helicopter Society*, 2015.
- [22] Q. T. Truong, H. V. Phan, S. P. Sane, and H. C. Park. Pitching Moment Generation in an Insect-Mimicking Flapping-Wing System. *Journal of Bionic Engineering*, 11(1):36-51, 2016.
- [23] H. V. Phan, and H. C. Park. Generation of Control Moments in an Insect-like Tailless Flapping-wing Micro Air Vehicle by Changing the Stroke-plane Angle. *Journal of Bionic Engineering*, 13(3):449-457, 2016.
- [24] H. V. Phan, T. K. L. Au, H. C. Park. Clap-and-fling mechanism in a hovering insect-like two-winged flapping-wing micro air vehicle. *Royal Society Open Science*, 3:160746, 2016.
- [25] H. V. Phan, and H. C. Park. Design and evaluation of a deformable wing configuration for economical hovering flight of an insect-like tailless flying robot. *Bioinspiration & Biomimetics*, 13:036009, 2018.
- [26] S. Aurecianus, H. V. Phan, N. S. Lok, T. Kang, and H. C. Park. Flapping wing micro air vehicle (FW-MAV) state estimation and control with heading and altitude hold. In *10<sup>th</sup> International Micro Air Vehicle Competition and Conference (IMAV)*, 2018.
- [27] T. Hedrick. Software techniques for two- and three-dimensional kinematic measurements of biological and biomimetic systems. *Bioinspiration & Biomimetics*, 3:034001, 2008.